Theoretical feasibility study on neutron spectrometry with the polyallyldiglycol carbonate (PADC) solid-state nuclear track detector

D. Nikezic [a,b], K.N. Yu [b,*]

[a] Faculty of Science, University of Kragujevac, R. Domanovica 12, Kragujevac 34000, Serbia
[b] Department of Physics and Materials Science, City University of Hong Kong, Tat Chee Avenue, Kowloon, Hong Kong

ARTICLE INFO

ABSTRACT

Neutron spectrometry with the polyallyldiglycol carbonate (PADC) film detector was analyzed in detail. The computer codes TRACK_TEST and TRACK_VISION, which were originally developed for studies on alpha-particle tracks, were modified to compute parameters of etched proton tracks developed in the PADC film detector and to simulate their appearance under an optical microscope in the transmission mode. It was shown that protons with same energy and recoil angle could produce different etched tracks with various size and shape, depending on the point of their creation. As such, it was necessary to employ multiple etching, and to measure the removed layer thickness and to record the track appearance after each etching step. A new variable, namely, the effective removed layer h_{eff}, was introduced as the difference between the total removed layer and the depth where the proton was created in the detector. A program modified from the TRACK_VISION code was used to plot the appearance of a number of representative etched proton tracks. For proton energies larger than 2 MeV, the V function for protons in PADC was found to be almost constant, so the simple formulas for major and minor axes of proton track openings could be used to determine the proton energy, recoiled angle as well as the energy of the neutron which caused the proton recoil. For lower proton energies, a databank of various proton tracks showing the track opening appearances and the track profiles should be created for comparison to facilitate the determination of the proton energy.

© 2014 Elsevier B.V. All rights reserved.

1. Introduction

It has been shown that detection and dosimetry of fast neutrons are possible with solid-state nuclear track detectors (SSNTDs). For this purpose, some converters can be placed between the neutron source and the SSNTD to facilitate the production of recoiled protons in the converter, which are further registered in the SSNTD [1–3]. However, under such a condition, most information on the energy of the incident neutron will be lost. As such, it is valuable and pertinent to explore alternative methods to be able to record and reconstruct the energy of the incident neutrons [4].

To be able to reconstruct the incident neutron energy spectra, it would be necessary to determine the energies of a large number of protons which produced the visible etched tracks in the detector.

However, this task was challenging because of the reasons explained in the following.

Fig. 1 shows a schematic diagram illustrating the special case where three neutrons, n_A, n_B and n_C with same energy, interact with the detector material at different depths, z_1, z_2 and z_3, and produce three protons with the same recoiled angles and the same energies. The latent tracks left behind by the three protons generated from the three neutrons, n_A, n_B and n_C, are labeled as A, B and C, respectively. As the etching proceeds, the new detector surface after etching will always move parallel to the original surface. After a certain thickness of the detector has been removed by etching, the etchant will have reached the starting point of the latent track A and will start developing this track, while the starting points of the latent tracks B and C have not yet been reached by the etchant. Further etching will enlarge the latent track A to become visible, and will also allow the etchant to reach the latent track B and will start developing this track, while the starting point of the latent track C has not yet been reached by the etchant. For prolonged etching, there will be three different etched tracks with very different size and shape. From this simplified

* Corresponding author. Tel.: +852 34427812; fax: +852 34420538.
  E-mail addresses: dnikezic@yahoo.com (D. Nikezic),
peter.yu@cityu.edu.hk (K.N. Yu).
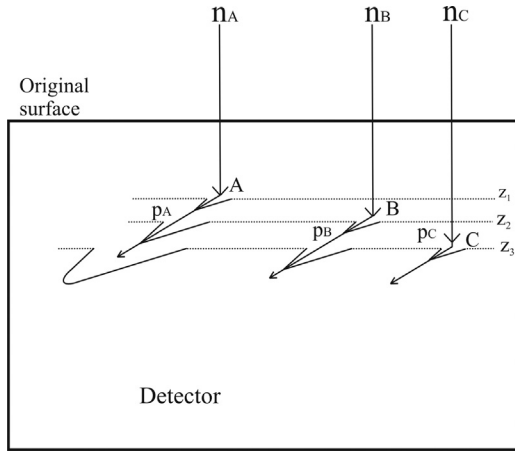
Fig. 1. Schematic diagram illustrating the special case where three neutrons, n_A, n_B and n_C with same energy, interact with the detector material at different depths, z_1, z_2 and z_3, and produce three protons with the same recoiled angles and the same energies.

description, it can already be concluded that track parameters cannot be directly used for determining the energy of the recoiled protons, which renders the reconstruction of the initial neutron energy spectra implausible.

The missing information is the depth z_{start} at which the tracks start to develop (viz., z_1, z_2 and z_3 in the previous text). To facilitate our discussion, we introduce the effective removed layer for each of track h_{eff} which is defined as $(h - z_{start})$, where h is the total removed layer during etching. This means that we might have to monitor the etching process in some way. For example, this can be realized by marking the detector surface into many rectangles using a mask. Multi-step etching is then applied with careful control of the removed layer. After each etching step, each rectangular region will be examined in detail to search for newly formed tracks, in addition to measuring the parameters of the etched tracks which have appeared earlier. This is certainly a tedious procedure but a knowledge on z_{start} appears to be indispensable for meaningful analyses of etched tracks.

In the present study, we performed a theoretical feasibility study on neutron spectrometry with polyallyldiglycol carbonate (PADC) solid-state nuclear track detectors (commercially available as CR-39 detectors). As a preliminary study, we considered the situation where fast neutrons, with energies between 1 and 10 MeV, struck the PADC film with normal incidence. The neutrons interacted with the atomic nuclei in the detector, with the most important interactions being those with hydrogen nuclei, after which recoiled protons were created. These protons left behind latent tracks in the detector which could be made visible after appropriate chemical etching. The parameters of these etched tracks contained information on the proton energies, which were in turn related to the initial neutron energies.

2. Relevant information

2.1. Interactions between neutrons and protons

Some discussion on the interactions between neutrons and protons (hydrogen nuclei) will be required to describe the challenge. The energy of the recoiled proton E_p, the energy of the neutron E_n and the angle of recoil θ are related through the equation:

$$E_p = E_n \cos^2 \phi \tag{1}$$

where ϕ is measured with respect to the direction of the incoming neutron [5]. If we only consider normal incidence of the neutron on the detector, the angle between the proton trajectory and the detector

surface is $\theta = (\pi/2 - \phi)$. Fig. 2 shows some of the possibilities which are useful for understanding the results which will be presented later.

The protons which are generated with a smaller angle with respect to the neutron trajectory will have larger energies and longer ranges, and vice versa. The ranges are qualitatively presented in Fig. 2 with arrows, and quantitative plots are possible using Eq. (1). The proton labeled p_1 was generated by a head-on collision and will have an energy equal to the neutron energy before collision, while in general a proton labeled as p_i will take only a fraction of the neutron energy.

2.2. V function for tracks produced by protons in the PADC

The formation of tracks by protons in the PADC film detector is governed by the corresponding V function, where $V = V_t/V_b$, V_t is the etch rate along the track and V_b is the etch rate of the bulk detector [6]. In the literature, such a V function is available [7], which is related to the residual range R' for protons, that is,

$$V(R') = 1 + [A_1 \exp(-A_2 R') + A_3 \exp(-A_4 R')][1 - \exp(-A_5 R')] \tag{2}$$

where $A_1 = 0.4306$, $A_2 = 7.3736 \times 10^{-3}$, $A_3 = 1.0559$, $A_4 = 0.1072$ and $A_5 = 1.4120$. This V function is graphically presented in Fig. 3.
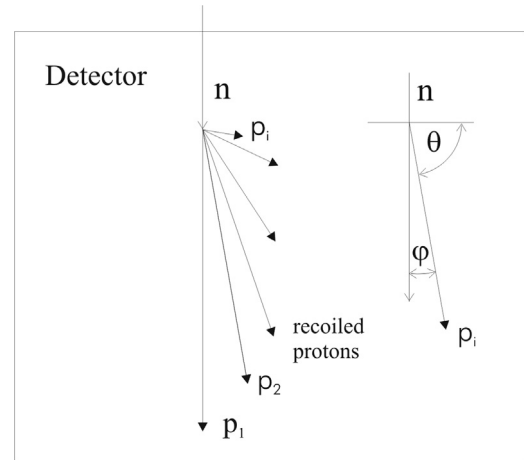
Fig. 2. Different possibilities for the recoiled protons. Note that the protons recoiled with a larger angle with respect to the neutron trajectory have smaller energies and shorter ranges in the detector. The meanings of angles θ and ϕ are shown on right.
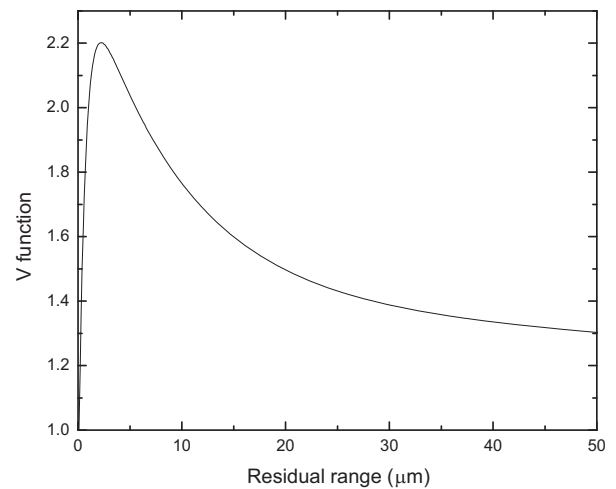
Fig. 3. V function for protons in the PADC film detector as a function of the residual range R', given by $V(R') = 1 + [A_1 \exp(-A_2 R') + A_3 \exp(-A_4 R')][1 - \exp(-A_5 R')]$, where $A_1 = 0.4306$, $A_2 = 7.3736 \times 10^{-3}$, $A_3 = 1.0559$, $A_4 = 0.1072$ and $A_5 = 1.4120$.

In Fig. 4, the range of protons in the PADC film detector material is presented as a function of the proton energy. The ranges were determined using the freely available software SRIM2003 [8]. It is remarked that protons have significantly larger ranges in PADC than alpha particles with the same energy. In ref. [9], the V function for protons in PADC was presented as a function of the Restricted Energy Loss (REL), but the more convenient form is expressed here in Eq. (2).

From Fig. 3, we can see that the V function does not vary significantly when the residual range reaches about 50 μm. From Fig. 4, this residual range corresponds to protons with energy of about 2 MeV. This means that the formulas derived for track parameters for a constant V function can be valid for protons with energy larger than 2 MeV, which can significantly simplify the analysis for cases with proton energy larger than 2 MeV.

2.3. Cross section for production of recoiled protons

For fast neutron spectrometry with PADC film detectors, the cross section for production of recoiled protons is required. The elastic scattering cross-section between neutron and proton is shown in Fig. 5 [10]. The cross section decreases considerably with increasing neutron energy. Higher-energy neutrons will interact by other processes, such as inelastic excitation of nuclei of constituent elements in the detector, or they do not interact at all.
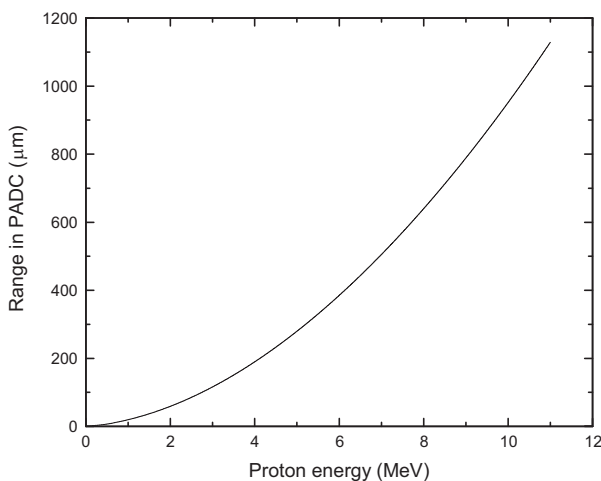
Fig. 4. Proton range in the PADC film detector as a function of proton energy. Protons with incident energies of 1 and 5 MeV have ranges of ∼19.5 and 279 μm, respectively. Calculated with SRIM2000.
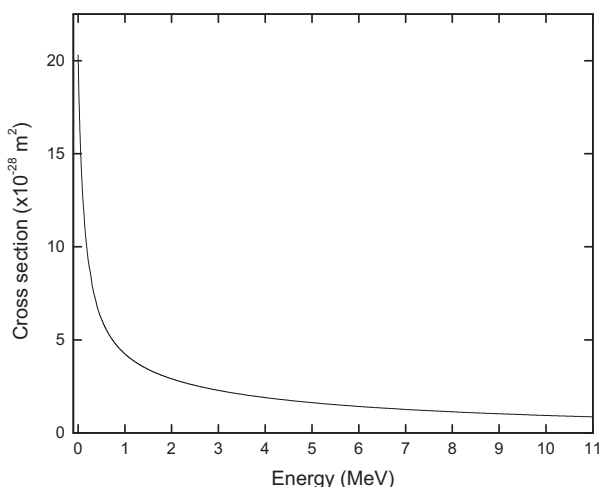
Fig. 5. Elastic scattering cross-section between neutron and proton (n,pn').

3. Characteristics and parameters of proton tracks in PADC film detector

Through the analyses of the proton ranges, recoil angles and the V function, some characteristics of proton tracks can be qualitatively understood and predicted. As an example, we consider the proton p_1 as depicted in Fig. 2. This proton has the largest possible energy which is equal to the initial neutron energy. Such a proton will also have the largest range, and the value of the V function is just barely larger than unity. In the lower-energy region considered here, that is, below 2 MeV, and with a small removed layer, the resulted track will have a sharp tip and its appearance under an optical microscope in the transmission mode will be completely black. When the removed layer increases, the track profile will become rounded and, under an optical microscope in the transmission mode, a bright portion will appear at the centre of the track and will increase in size. Finally, after sufficient etching, the track appearance under the microscope will lose its black part and become entirely bright. Examples are shown in Fig. 6, where evolution of the profiles and appearances of the tracks generated by protons with an energy of 1 MeV produced with an angle of 90° with respect to the detector surface are shown (first column).

On the other hand, higher-energy protons, which can be created in head-on collisions with higher-energy neutrons, have longer ranges and thus smaller values of the V function at the sites where the tracks start developing. As such, the corresponding track openings will be wide while total internal reflection will not occur when light strikes the bottom of the tracks, so the entire track will be bright with only small attenuation in the light intensities. By increasing the removed layer, the size of the track will increase, but in general no black portions will appear under the microscope. For the black portion to emerge, etching must proceed along the track to reach several ten micrometers from the end of range of the protons. An example is given in Fig. 6 for 5-MeV protons under an incidence of 90°. Such tracks are very shallow and provides very weak contrast so these tracks are difficult to observe and will be missed in most analyses.

The third and fourth columns in Fig. 6 correspond to smaller incident angles for the recoil protons. In these cases, some egg-like or drop-like track openings are obtained, which will depend on the energy and incident angle of the recoil protons.

The last column in Fig. 6 refers to cases with very large removed layers, namely, 160 and 200 μm, which may not be feasible in practical applications. Protons with an energy of 6 MeV have a range of about 385 μm in PADC. The value of the V function for such a large residual range is very small, and close to unity, so a small deviation of the incident angle from normal incidence (90°) will disable the track development because the condition $V\sin\theta > 1$ is not satisfied. When the removed layer h increases, the etchant is moving toward the region in the latent track with larger values of the V function. For a certain value of h, the condition $V\sin\theta > 1$ will become satisfied and the track development starts.

We next consider the tracks p_i in Fig. 2. Here, the protons are emitted with a large angle with respect to the neutron direction, or in other words a small angle with respect to the detector surfaces. These protons have small energies, so the corresponding values of the V function can be sufficiently large to start the track development. Such tracks will be very shallow, without a black portion in their appearance and without good contrast, so these tracks can be missed from analysis.

The images presented in Fig. 6 were obtained using computer codes modified from our previously developed computer codes called TRACK_TEST [11] and TRACK_VISION [12]. The previous computer codes were originally developed for alpha-particle irradiation, and were now modified to include stopping power and
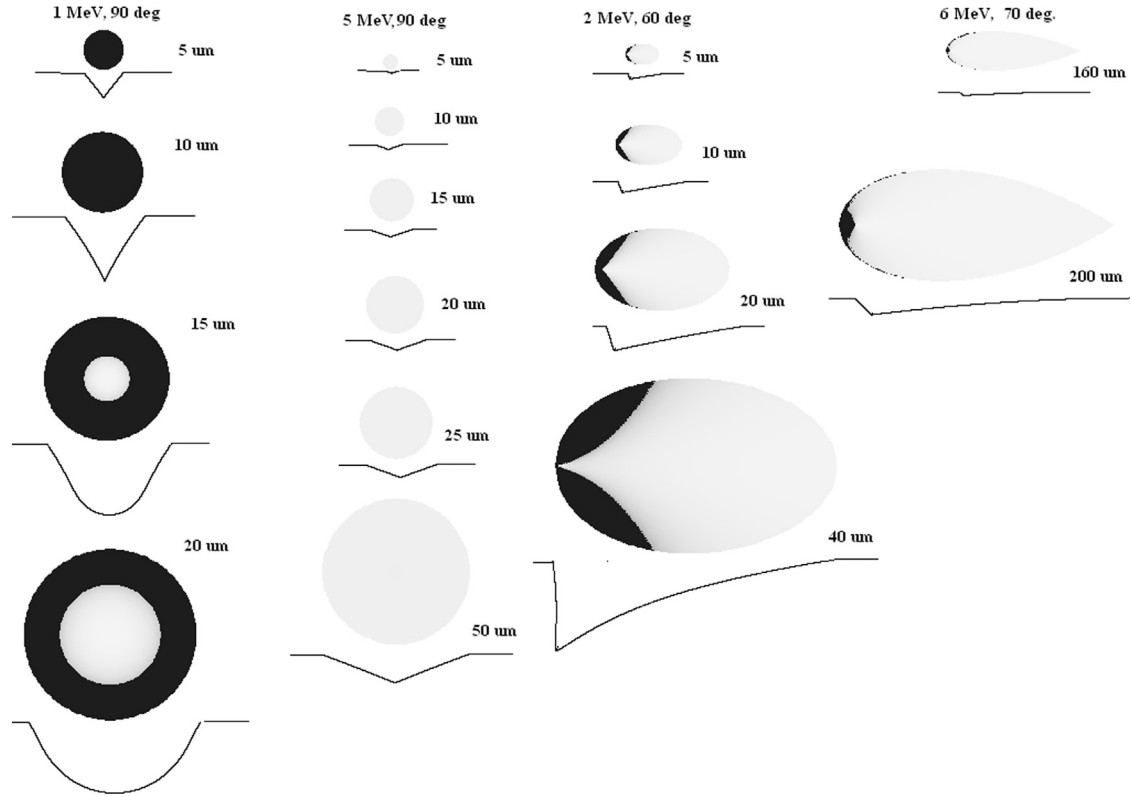
Fig. 6. Examples of profiles and track appearances under an optical microscope in the transmission mode obtained for tracks formed by protons with different energies (produced with an angle of 90° with respect to the detector surface). The thickness of removed layers h_{eff} are also shown.

ranges of protons in the PADC film detector to allow studies on proton tracks. To distinguish from the previous program TRACK_VISION, the new version was referred to as TRACK_VISION_P (where P signified the version dedicated to studies on protons).

Modifications to our previous computer code included the following. First, the data on stopping powers and ranges for alpha particles were now replaced by the corresponding data for protons (both obtained from the software SRIM2003 [8]). Second, the V function for alpha particles was now replaced by the V function for protons as given by Eq. (2). Third, in the previous version of our TRACK_VISION program, track images were scaled in such a way that all tracks had similar size on the computer screen. The real size and parameters of the tracks could then be determined by the users using the scale bar provided on left side of the computer screen. In the new version of the program, which was used in the present work and which was dedicated to proton-track simulation, scaling of track images was disabled by default and the computer screen represented a real-life area with the same size, except in cases where the track was too large to fit onto the computer screen. The program set the screen with a horizontal-vertical aspect ratio of 4:3, which corresponded to resolutions of, for example, 800:600 or 1024:768 etcetera. Using other aspect ratios would distort the track appearance, for example, a circular track obtained from a normally incident particle could become elliptical. If the track became too large to fit onto the computer screen, which might occur when the removed layer was very large, the computer program provided an option for the user to switch on the scaling, but with the aspect ratio of 4:3 preserved. When scaling was switched on, the area represented by the computer screen would be displayed.

As mentioned above, protons with energies larger than 2 MeV have ranges longer than 50 μm in PADC film detectors. For these proton energies, the corresponding V function was almost constant and the formulas for the major axis D and the minor axis d

derived under constant V could be valid [13], where

$$D = 2h\left(V^2 - 1\right)^{1/2} / (V \sin \theta + 1) \tag{3}$$

and

$$d = 2h[(V \sin \theta - 1)/(V \sin \theta + 1)]^{1/2} \tag{4}$$

From Eqs. (3) and (4), through elimination of the angle θ, V could be expressed as

$$V = \left[\left(16D^2 h^2\right) / \left(4h^2 - d^2\right)^2 + 1\right]^{1/2} \tag{5}$$

For example, a proton with energy $E = 3$ MeV and an incident angle of 75°, upon etching an effective removed layer of 10 μm, will produce a track with $D = 5.96$ μm and $d = 5.226$ μm (calculated using TRACK_VISION_P). Substitution of these data in to Eq. (4) will give $V = 1.187$. From the $V(R')$ function, we can numerically determine $R' = 113$ μm, which correspond to the energy of 2.955 MeV (from Fig. 4), which is very close to the proton energy of 3 MeV. Agreement will be even better for higher energies because the variation of the V function is even smaller along the generated proton tracks. However, if a very thick removed layer is etched away (e.g., 160 μm as shown in the 4th column in Fig. 6), although the variation of V is small, it might become significant and lead to errors up to 1 MeV in the estimation of proton energy.

Furthermore, we can use Eq. (4) (or Eq. (3)) to determine the angle of proton incidence as

$$\sin \theta = \left(4h^2 + d^2\right) / \left(4h^2 - d^2\right) / V \tag{6}$$

For example, calculations with TRACK_VISION_P for input parameters: proton energy $E_p = 6$ MeV, incident angle $= 80°$ and removed layer $= 50$ μm, will produce the following data: $D = 11.795$ μm and $d = 7.8037$ μm. From Eqs. (5), $V = 1.0278$ and from $V(R')$, $R' = 372$ μm which corresponds to $E_p = 5.88$ MeV. Using Eq. (6), the estimated

angle is $\theta = 80.03°$. On knowing the energy and incident angle of the proton, we can determine the neutron energy which generate that recoiled proton using Eq. (1), that is, $E_n = E_p/\cos^2\phi = 5.88/\sin^2\theta = 6.062$ MeV.

4. Conclusion

Neutron irradiation of the PADC film detector will create a variety of recoil-proton tracks, with the track opening shape, size and parameters, as well as the fraction of the black portion observed under the optical microscope depending on the incident proton energy, angle of recoil, removed layer and starting point z_{start} of the latent track.

When the protons have energies larger than 2 MeV, measurements of the major and minor axes of the proton-track openings can help determine the proton energy, the recoiled angle and also the neutron energy. It is, however, remarked that such capabilities have to rely on the small variation of the V function when the residual range is larger than 50 μm (or correspondingly the protons have energies larger than 2 MeV).

On the contrary, for lower proton energies, the V function vary considerably, so the approach described above for higher proton energies cannot be applied. As such, as regards lower proton energies, the determination of the energies of the protons, which are needed to reconstruct the neutron energy spectrum, requires a databank of track profiles and track appearances under an optical microscope in the transmission mode obtained for a large number of tracks formed by protons with different energies, with examples shown in Fig. 6. With this databank, real tracks obtained from experiments can be compared with those in the databank for matching. In this way, the energies of the protons can be determined.

The remaining problem is how to differentiate between the tracks created from high- and low-energy protons. An empirical rule can be inferred from Fig. 6, where lower-energy protons will produce tracks with larger black portions while higher-energy protons will produce brighter tracks with smaller black portions closer to the particle track.

References

[1] M. Caresana, M. Ferrarini, A. Pola, S. Agosteo, F. Campi, A. Porta, Nucl. Instrum. Meth. A. 620 (2010) 368.
[2] F. Castillo, G. Espinosa, J.I. Golzarri, D. Osorio, J. Rangel, P.G. Reyes, J.J.E. Herrera, Radiat. Meas. 50 (2013) 71.
[3] A.R. El-Sersy, Nucl. Instrum. Meth. A. 618 (2010) 234.
[4] S. Paul, S.P. Tripathy, G.S. Sahoo, T. Bandyopadhyay, P.K. Sarkar, Nucl. Instrum. Meth. A. 729 (2013) 444.
[5] K.N. Mukhin, Experimental Nuclear Physics, Mir, Moscow, 1987.
[6] D. Hermsdorf, Radiat. Meas. 44 (2009) 806.
[7] D. Nikezic, K.N. Yu, Mater. Sci. Eng. R. 46 (2004) 51.
[8] J.F. Ziegler, J.P. Biersack, M.D. Ziegler, SRIM – The stopping and range of ions in matter, SRIM Co. ⟨http://www.srim.org⟩, 2012.
[9] B. Dorschel, D. Hermsdorf, K. Kadner, S. Starke, Radiat. Meas. 35 (2002) 287.
[10] T-2 Nuclear Information Service, ⟨http://t2.lanl.gov/⟩, (last accessed 25.08.14).
[11] D. Nikezic, K.N. Yu, Comput. Phys. Commun. 174 (2006) 160.
[12] D. Nikezic, K.N. Yu, Comput. Phys. Commun. 178 (2008) 591.
[13] G. Somogyi, S.A. Szalay, Nucl. Instr. Meth 109 (1973) 211.